FAST 3D OPTICAL-PROFILOMETER FOR THE SHAPE-ACCURACY CONTROL OF PARABOLIC-TROUGH FACETS

Marco Montecchi[1], Arcangelo Benedetti[2], and Giuseppe Cara[3]

[1] Researcher physicist at ENEA CR Casaccia, Via Anguillarese 301, 00123 S. Maria di Galeria (Roma), Italy.

Phone: +39 06 3048 3587 email: marco.montecchi@enea.it

[2] Electronic technician at ENEA CR Casaccia, Phone: +39 06 3048 6385

[3] Electronic technician at ENEA CR Casaccia, Phone: +39 06 3048 6380

Abstract

The VISprofile is an innovative instrument for verifying the shape-accuracy of parabolic-trough facets. Simplicity and low-cost are two strengths of the new instrument, being composed by only three components, of which the linear guide rail is the most expensive. VISprofile allows measuring not only the partial derivatives ∂z/∂x and ∂z/∂y, but also the profile (*z* coordinate) of the facet surface; therefore, differently from the concurrent instruments, VISprofile can be categorized as *profilometer*. Moreover, VISprofile exhibits superior accuracy: about 20 μrad and 50 μm for derivatives (arctangent) and *z* deviation (from the ideal shape), respectively. The proposed instrument is suitable for the industrial quality-control, the total measurement time (data processing included) being about 1 min/m^2, with a sampling-density of 1 point/cm^2.

Keywords: Solar-concentrator, Reflector, Facet, Profilometer, Intercept-factor.

1. Introduction

The effectiveness of solar concentrators strongly depends on the shape accuracy of the reflective panels (facets) that compose it. ENEA developed a high precision optical profilometer (OP) [1] for in-laboratory characterization, which was intensely used during the R&D of reflective parabolic-trough panels of several Italian producers.

The instrument allows to measure the panel surface in terms of its *x*,*y*,*z* coordinates together with the partial derivatives, ∂z/∂x and ∂z/∂y, with high accuracy: 20 μm and 15 μrad for *z* deviation and derivatives, respectively. Then, by means of ray tracing, a number of figures (the most representative being the intercept factor) are evaluated. Although OP has some similarity with V-SHOT [2], OP differs from it in several important respects; the most noticeable is the data-processing method which allows to measure not only the partial derivatives, but also the *z* coordinate.

Unfortunately OP is not suitable for the industrial quality control because of the quite long measuring time (about 1h/m^2). For that purpose, actually the most reliable technique is the Fringe Reflection Technique (FRT) [3]; but this technique, like V-SHOT, allows to measure only the partial derivatives ∂z/∂x and ∂z/∂y (with 1 mrad accuracy, that is worst than OP), but not the *z* coordinate. Even if concentration-effectiveness is dominated by derivative-deviations (i.e. the difference from that of the ideal shape), the *z*-deviation knowledge is generally more useful for the manufacturing-process optimization.

Recently we developed a completely new technique: the Visual Inspection Method (VIM) [4]. Based on VIM, now two innovative VIS (Visual Inspection System) instruments are commercialized by MARPOSS [5] under ENEA license:

- VISfield [6], for in field measuring: i) intercept factor of a whole module (usually, 12 m long), ii) optimizing facet-orientation and iii) final checking of facet-shape compliance. All these features make VISfield more performing than TOPCAT [7], its main concurrent.
- VISprofile, fast 3D optical profilometer for laboratory/industrial quality-control of parabolic-trough facets.

The latter is the topic of this paper.

2. VISprofile

2.1. Theory

The VIM is based on the principle of ray reversibility, also known as the reciprocity theorem of Helmholtz [8]; this principle states that any ray of light in an optical system, if reversed in direction, will retrace the same path backwards. This suggests investigating the performances of solar concentrators in reverse: placing a suitable light source instead of the receiver and observing the results from the Sun point of view. The requirement to observe the panel from so large distance seems to make VIM hardly applicable. However, this limit can be overcome with the help of a consideration: the far-field image can be reconstructed by processing a large enough number of images taken in the near field from different observation points [4].

According to the VIM approach, let S be a point light source on the focus line of a parabolic-trough facet, $S=(x_S, y_S, z_S)$. As shown in Fig. 1, the observer C is set in front of the reflective surface in $C=(x_C, y_C, z_C)$ and sees S imaged in the point $P=(x, y, z)$ of the facet surface. As will be discussed in sub-paragraph 2.4, the observer can evaluate (x, y) by referring to: i) facet width *L*, ii) camera abscissa x_C and iii) camera aiming; on the contrary *z*-evaluation needs a more complex procedure which is explained in sub-paragraph 2.2.

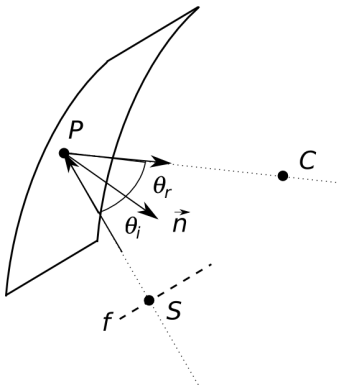

Fig. 1. The observer *C* sees the point light source *S* imaged in *P* of the parabolic-trough facet-surface; position and normal to the surface in *P* have to fulfill the two reflection laws

Anyway, given the position of S and C, position and normal to the surface in P have to fulfill the two reflection laws [8], summed up by the equation

$$-\overrightarrow{SP}+\overrightarrow{PC}\propto\vec{n} \qquad [1]$$

where all the vectors are unit vectors, and $\vec{n}$ is normal to the facet surface in P.

It is easy to verify the relationship between $\vec{n}$ and the partial derivatives of the surface in P:

$$\vec{n}\propto\left(\frac{\partial z}{\partial x},\frac{\partial z}{\partial y},-1\right) \qquad [2]$$

2.2. Data processing

The schema of the experimental apparatus will be described in sub-paragraph 2.3. For now let us discuss the processing of the acquired experimental-data-set, composed by terns of (S, P, C), arranged in such a way that the ensemble of P points draws a sort of regular grid across the whole facet-surface.

Let P_0 be a point of the facet-surface of which *z* is known. On the basis of Eqs. 1 and 2, the derivatives ∂z/∂x and ∂z/∂y are uniquely determined by the experimental tern (S, P_0, C).

Now, among the neighbor points of P_0, let us consider P_1 (see Fig. 2); here z_1 is not known. On the other hand, if the grid-step is short enough to assume the behavior of the derivatives as monotonic, for an ideal parabolic profile, the planes tangent in P_0 and P_1 are expected to intersect one each other at midway [1],

$$x_i = (x_0 + x_1)/2 \qquad [3a]$$

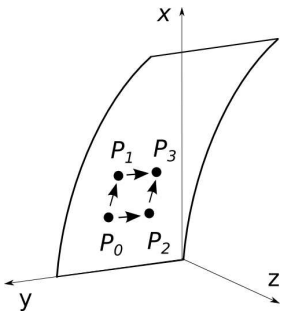

Fig. 2. Some neighborhoods of P_0 and paths along which to extend *z* and derivatives knowledge.

It is reasonable to extend this criterion also along y; therefore considering the neighbor point P_2, the intersection of the planes tangent in P_0 and P_2 is expected in

$$y_i = (y_0 + y_2)/2 \qquad [3b]$$

In both cases $P_0 \rightarrow P_1$ and $P_0 \rightarrow P_2$, the midway criterion together with Eqs. 1 and 2 allows to uniquely evaluate z, ∂z/∂x and ∂z/∂y in the neighbor points of P_0.

Concerning the neighbor point P_3, placed obliquely, it can be reached from P_0 by the two different paths $P_0 \rightarrow P_1 \rightarrow P_3$ and $P_0 \rightarrow P_2 \rightarrow P_3$; in this case the average of the two results is considered.

By the iterative application of this procedure, z, ∂z/∂x and ∂z/∂y can be evaluated over the whole facet-surface.

At first glance this procedure could appear trivial, equivalent to $z = z_0 + \sum \frac{\partial z}{\partial r} \Delta r$, but it is not so because the value of the partial derivatives given by Eqs. 1 and 2 depends on *z* itself, making a standard numerical integration method unusable. On the other hand, the above formula suggests a quite simple way for error evaluation: $Err(z) = Err(z_0) + \sum Err(\frac{\partial z}{\partial r}) \Delta r$.

Once the facet surface is known, then several features are evaluated by ray tracing , ranging from the intercept factor to the radiation flux on the receiver surface; in all cases, the divergence of the solar radiation is taken into account.

2.3. Experimental schema

The VISprofile is sketched in Fig. 3 together with the adopted reference system. The three main components: i) linear array of point light sources, ii) camera, and iii) motorized linear guide rail, are conveniently aligned with respect to the facet.

The source array is placed along the nominal focus line of the parabolic-trough facet under test; in this manner, for perfectly shaped reflectors, the observer C sees the point-source images, aligned across the panel width (in the flat direction, y axis), at his own abscissa, i.e. $x = x_C$. Otherwise, shape imperfections in the curved direction (x axis) result in displacement of the point-source images from x_C.

The array length is set so that the camera views the point-source images spread across the entire panel width *L*.

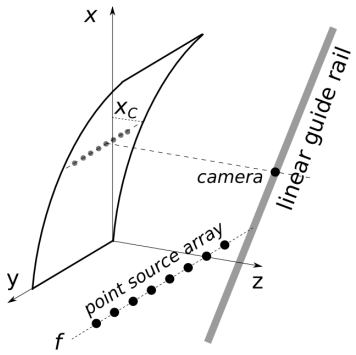

Fig. 3. VISprofile sketch

The camera is installed on the motorized linear guide rail, which is placed centrally in front of the specimen, and oriented parallel to the facet chord in order to reduce the variation of the distance of the camera from the facet, $d = z_C - z$ experienced during the specimen-scanning.

The scan consists of grabbing a number of frames varying the camera abscissa, so that during the scan the observed point-source-images span the whole facet-surface, from one linear edge to the opposite one. For this purpose the rail length must be a bit longer (typically 20%) than the chord because shaping-imperfections make the optimal scan-range wider.

The number of point-sources and the x_C -step between one frame and the following are chosen so as to ensure a sufficient sampling density over the facet surface.

After the scan, the collected data are irregularly spaced in XY plane. For both graphical and statistical reasons, regularizing that mesh with a gridding method [9] is convenient.

2.4. Procedure for camera alignment and image calibration

This issue is fundamental for the correctness of the results achieved with the VISprofile. In the following, image distortion due to the objective as well as pitch, roll and yaw of the camera on the linear guide rail are considered negligible; otherwise each one of these imperfection can be easily correct via software.

The procedure for camera alignment and image calibration basically consists of two steps:

• Move the camera at $x_C = 0$; adjust yaw and roll, respectively, centering the image of the source-array and aligning it with the CCD rows; let $j0$ be the pixel-row number along which the point-sources appear disposed.

• Move the camera at the facet minimum-abscissa $x_C = x_{min}$; adjust the objective focal-length to grab the full linear edge of the specimen.

Henceforth the real coordinates of any point on the facet surface can be evaluated from its pixel coordinates (ξ, η). As a matter of fact, with good approximation the distance from the camera to the point $(x_C, L/2, z)$ of the facet surface, is given by

$$d = z_C - z = z_{C0} + a x_C - x_C^2/(4\mathrm{f}) \qquad [4]$$

being $C = (x_C, L/2, z_{C0} + a x_C)$ and the parabolic-trough profile $z = x_C^2/(4\mathrm{f})$.

Let $N_W \times N_H$ be the image resolution; due to the fact that lens work in para-axial approximation, and the camera sensor is oriented parallel to the facet-surface in the y direction (by way of the above procedure), along the row $j0$ the image is composed by pixels covering the same step of the facet-surface

$$\Delta_{j0} = \frac{L}{N_W}\frac{d_0}{d} \qquad [5]$$

where d_0 is the distance at $x_C = x_{min}$.

Conversely, along the x axis, facet and camera-sensor surfaces are oblique one to each other, and the grabbed image is affected by the falling lines phenomenon; as a consequence, the step of the facet-surface covered by one pixel changes row by row and it has to be computed starting from $j0$ by the iterative application of Eq. 5 considering the off-optical-axis distance

$$d = z_C - z = z_{C0} + ax_C - x_j^2/(4\mathrm{f}) \qquad [6]$$

where j =int (η) .

With a few mathematical steps we get

$$x_j = x_c \pm \sum_{j=j0}^{j\mp1} \Delta_j \qquad [7]$$

where upper and lower signs hold for $j < j0$ or $j > j0$, respectively. Please note that, as conventionally assumed, the upper left corner of the digital image is the origin of the pixel reference system.

Therefore,

$$x = x_j - (\eta - j)\Delta_j \qquad [8a]$$

$$y = (\xi_R - \xi)\Delta_j \qquad [8b]$$

where ξ_R is the pixel-coordinate of the right facet-edge given by

$$\xi_R = \frac{N_W}{2}\left(1 + \frac{d}{d_0}\right) \quad . \qquad [9]$$

3. Experimental

The linear array of point light sources is simply made with a linear fluorescent Neon lamp enclosed in a metallic extrude, of which one face is suitably drilled (see Fig. 4). The array length is set to 1500 mm, so that from 6 meter away the point-source images appear spread over 1200 mm, that is the width (along the y axis) of the facets developed during the R&D of the Italian CSP project. The observation distance is set to 6 m to allow to measure the facet with both VISprofile and the older OP; this makes the comparison of the results achieved with these two instruments more rigorous.

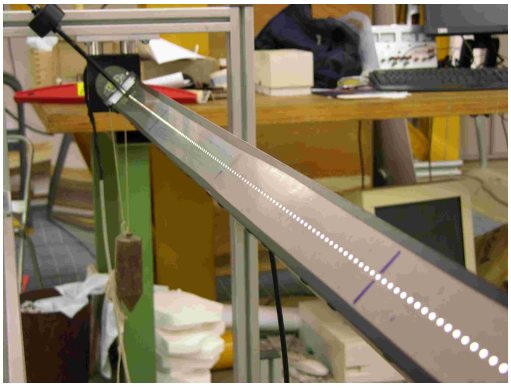

Fig. 4. Linear array of point light source

From previous studies we found that the iterative data-processing method described in sub-paragraph 2.2 is

certainly reliable when the sampling-density is not lower than 1 point/cm^2 [1]; for this reason the number of point light sources and x_C -step are set to 151 and 1 cm, respectively.

As shown in Fig. 4, the lamp envelope is hung to a frame by two joints, which let us free to orient the drilled face towards the specimen as well as the camera (the latter is essential during the calibration procedure).

Fig. 5. Hamamatsu C8484-05G on the motorized linear guide rail

The motorized linear guide rail is 4 m long and supports a FireWire camera Hamamatsu C8484-05G (1344×1024) equipped with a Nikkor AF 28-105 mm 1:3.5-4.5 D (see Fig. 5).

Facet, source array, and rail were positioned by means of a total station Leica TDA5005.

Data acquisition and processing are controlled with a custom software written in C++, using the open source libraries libdc1394 and openCV; the GUI was written in Qt4. Measurement and data processing for panels shaped as half parabolic-trough (chord 3m) with sampling-density of 1 point/cm^2 takes about 2 min. It is noteworthy that this very good results are made possible by the FireWire connection and the C++ programming.

Concerning image-distortion due to the objective and roll, pitch and yaw induced by the rail, only pitch and yaw are significant, and they are properly taken into account during the image analysis.

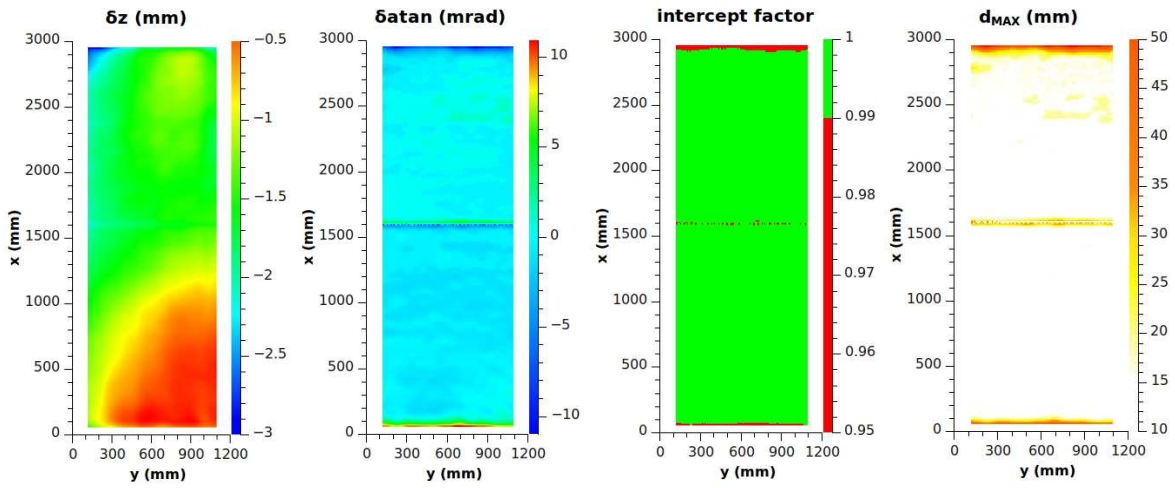

Fig. 6. Main graphical outputs achieved with the VISprofile on a facet shaped as half-parabola; from left to right, z-deviation, ∂z/∂x-deviation, intercept factor, and maximum distance from the focal line of the reflected solar-beam. The solar divergence is taken into account.

As an example, Fig. 6 shows the main graphical outputs achieved with the VISprofile for a panel shaped as half-parabola, width 1200 mm and aperture 3000 mm about. As expected, the concentration effectiveness of the facet, well represented by the intercept-factor (i.e. the ratio of the rays reflected towards the receiver and geometrically captured by it) as well the maximum distance from the focal line of the reflected solar beam

(divergence included), is mainly dominated by ∂z/∂x deviation. The most deviating regions are the neighborhoods of the linear edges and the central horizontal border between the two thin sheet glass mirrors composing the reflecting surface.

The z-deviation graph gives direct information on how to optimize the manufacturing process; in the example, the facet-surface is depressed of about 3 mm in the neighborhood of the left upper-corner.

Beside maps, the VISprofile data-processing software provides several important averaged values, one for all the mean intercept factor, 99,2% for the above facet. All these numbers are conveniently collected in a data-base.

Concerning the experimental errors, the positioning accuracy of facet, array and rail is 0.3 mm (rms), that is the one provided by the total station Leica TDA5005. Referring to Eqs. 1 and 2, this value is the positioning accuracy of *S* and *C*; it is noteworthy that these are systematic errors. Instead *P* is affected by a random error due to the centroid evaluation of the spot made by the point-light-source image; this is approximately 0.1 pixel, a spot-diameter being few pixel tenths wide. The error on the (x,y) coordinates of P is about 0.1 mm. The relative error of the arctangent of the derivatives ranges from 14 μrad, at x=0, to 22 μrad, at x=3000 mm. Finally, the error on *z* deviation increases almost linearly with the distance from P_0, the point from which the iterative method starts; in the actual example it increases up to around 50 μm.

We compared VISprofile and OP by measuring the same sample in the same conditions: the achieved results were always in very good agreement. With respect to OP, VISprofile offers a much faster measuring time (about 300 times); this allows to set the sampling-density on x and y uniform. On the contrary, to limit the measuring time, with OP the sampling-density on y has to be set to 1/5 of that on x.

5. Conclusion

The VISprofile is an innovative instrument to verify the shape-accuracy of parabolic-trough facets. The new instrument is characterized by simplicity and low-cost, being composed by only three components of which the most expensive is the linear guide rail. It allows to measure not only the partial derivatives ∂z/∂x and ∂z/∂y, but also the profile (*z* coordinate) of the facet surface, therefore the VISprofile belongs to the profilometric instrument class. The same can not be claimed by the most popular instruments, such as V-SHOT and FRT instruments. Moreover, with respect to those instrument, the VISprofile exhibits a superior accuracy: about 20 μrad and 50 μm for arctangent of derivatives and *z* deviation, respectively.

For facets shaped as half-parabola, width 1.2 m and aperture 3 m, the total measurement time, including data processing, is about 2 minutes with a resolution of 1 point/cm^2. This makes the VISprofile suitable for the industrial quality-control.

References

[1] A. Maccari, M. Montecchi, Solar Energy 81 (2007) 185-194.

[2] T. J. Wendelin, G. J. Jorgensen, R. L. Wood, Solar Engineering 2 (1992) 971-980.

[3] T. Bothe, W. Li, C. Kopylow, W. Jüptner, Proc. FRINGE 2005 International Workshop (2005).

[4] Italian patent deposited on March 3rd , 2008 No. RM2008A000151.

[5] MARPOSS is a global supplier of precision metrology equipment, see www.marposs.com.

[6] M. Montecchi, A. Benedetti, G. Cara, paper 107, SolarPACES2010 Congress, Perpignan (F), September 21-24, 2010.

[7] TOPCAT Solar Cell Alignment & Energy Concentration Technology, U.S. Patent no 7,667,833 (2010).

[8] M. Born, E. Wolf, Principles of Optics, 7th ed., Cambridge University Press, Cambridge 2005.

[9] R. L. Renka, A. K. Cline, Rocky Mountain J. Math. 14 (1984) 223-237.